Published in final edited form as:

J Anat. 2018 January ; 232(1): 39–53. doi:10.1111/joa.12720.

Ontogeny of hallucal metatarsal rigidity and shape in the rhesus monkey (*Macaca mulatta*) and chimpanzee (*Pan troglodytes*)

Biren A. Patel[1,2,*], **Jason M. Organ**[3,4], **Tea Jashashvili**[5,6], **Stephanie H. Bui**[2], and **Holly M. Dunsworth**[7]

[1]Department of Integrative Anatomical Sciences, Keck School of Medicine, University of Southern California, Los Angeles, CA 90033 USA

[2]Human and Evolutionary Biology Section, Department of Biological Sciences, University of Southern California, Los Angeles, CA 90089 USA

[3]Department of Anatomy and Cell Biology, Indiana University School of Medicine, Indianapolis, IN 46202, USA

[4]Department of Biomedical Engineering, Indiana University – Purdue University Indianapolis, Indianapolis, IN 46202, USA

[5]Molecular Imaging Center, Department of Radiology, Keck School of Medicine, University of Southern California, Los Angeles, CA 90033 USA

[6]Department of Geology and Paleontology, Georgian National Museum, Tbilisi 0105, Georgia

[7]Department of Sociology and Anthropology, University of Rhode Island, Kingston, RI 02881 USA

Abstract

Life history variables including the timing of locomotor independence, along with changes in preferred locomotor behaviors and substrate use during development, influences how primates use their feet throughout ontogeny. Changes in foot function during development, in particular the nature of how the hallux is used in grasping, can lead to different structural changes in foot bones. To test this hypothesis, metatarsal midshaft rigidity (estimated from the polar second moment of area [*J*] scaled to bone length) and cross-sectional shape (calculated from the ratio of maximum and minimum second moments of area, *Imax/Imin*) were examined in a cross-sectional ontogenetic sample of rhesus macaques (*Macaca mulatta*; n=73) and common chimpanzees (*Pan troglodytes*; n=79). Results show the hallucal metatarsal (Mt1) is relatively more rigid (with higher scaled *J* values) in younger chimpanzees and macaques, with significant decreases in relative rigidity in both taxa until the age of achieving locomotor independence. Within each age group, Mt1 rigidity is always significantly higher in chimpanzees than macaques. When compared to the lateral metatarsals (Mt2–5), the Mt1 is relatively more rigid in both taxa and across all ages, however this difference is significantly greater in chimpanzees. Length and *J* scale with negative

[*]*Correspondence*: birenpat@usc.edu.

DR. BIREN A. PATEL (Orcid ID : 0000-0003-1844-1931)

Author Contributions

HMD conceived the study; BAP, JMO, TJ, SHB and HMD collected the data; BAP analyzed the data; BAP drafted the manuscript; all authors gave final approval for publication.

allometry in all metatarsals and in both species (except the Mt2 of chimpanzees, which scales with positive allometry). Only in macaques does Mt1 midshaft shape significantly change across ontogeny, with older individuals having more elliptical cross sections. Different patterns of development in metatarsal diaphyseal ridgidity and shape likely reflects the different ways in which the foot, and in particular the hallux, functions across ontogeny in apes and monkeys.

Keywords

hallux; ape; monkey; climbing; grasping; cross-sectional geometry

Introduction

Inter- and intraspecific differences exist in the ways primates use their hallux as a grasping organ during locomotion and other behaviors, and this has long been hypothesized to be reflected in its functional morphology (Conroy and Rose, 1983; Gebo, 1985; Szalay and Dagosto, 1988; Strasser, 1994; Goodenberger et al., 2015). For example, non-human primates that are perceived to use their big toes to grasp with greater force tend to have relatively longer and more robust hallucal metatarsals (Mt1s) (Conroy and Rose, 1983). These include taxa that habitually walk on narrow diameter arboreal substrates in contrast to those that walk on wider diameter branches or on the ground, as well as taxa that use more vertical climbing, grasp-leaping and hindlimb suspensory behaviors versus those that are predominantly quadrupedal (e.g., Cartmill, 1974, 1985; Conroy and Rose, 1983; Patel et al., 2017). In line with hypotheses proposed by Preuschoft (1970) based on theoretical analyses, one biomechanical rationale for this is that Mt1s used in habitual hallucal opposition and grasping should experience variable and greater mechanical loads than Mt1s that are used less frequently in these behaviors. These contrasting loading environments are likely caused, in part, by differential contraction of muscle-tendon complexes that move the hallux, in combination with larger bending moments that act on the diaphysis as the hallux opposes the other digits around a curved or uneven substrate. Therefore, with the potential for experiencing habitually greater bending moments there would be a need for greater structural rigidity. Some support for this comes from morphological studies exploring metatarsal cross-sectional geometric properties in apes that rely on a grasping hallux for diverse positional and locomotor behaviors (e.g., Marchi, 2005, 2010; Jashashvili et al., 2015).

Our understanding of the relationship between *in vivo* grasping performance (i.e., force production) and hallux morphology in primates, however, has been based primarily on indirect lines of experimental evidence since, at least to our knowledge, there are no published studies assessing hallux grasping strength using force transducers. For example, research using electromyography to investigate muscles that flex and adduct the hallux (Boyer et al., 2007; Kingston et al., 2010; Patel et al., 2015a, b) can only be used to generalize and make inferences about force magnitudes (e.g., Roberts and Gabaldón, 2008). The few early dynamic plantar pressure studies in non-human primates, most of which had been on flat, terrestrial substrates, described the magnitudes of pressure (and the vertical component of ground reaction force) acting on the hallux during locomotion, but these rarely

discuss specific bouts of grasping (Wunderlich, 1999; Vereecke et al., 2003; Higurashi et al., 2010; Hirasaki et al., 2010). More recently, however, plantar pressure analyses comparing terrestrial and above-branch quadrupedalsim with vertical climbing in chimpanzees have noted that the hallux experiences higher pressure-time integrals during the support phase of the two arboreal behaviors, thereby suggesting that the hallux is loaded more when used to grasp than when used as a weight-bearing strut (Wunderlich and Ischinger, 2017). Also during arboreal quadrupedalism in lemurids, the hallux appears to experience higher mean and maximal pressures than the lateral pedal digits (see Table 2 in Congdon and Ravosa, 2016). Overall, however, in the absence of more focused experimental data, alternative approaches are necessary to further understand the relationship between Mt1 morphology and hallucal grasping performance and behavior.

One approach to assess a potential biomechanical link between behavior and skeletal structure is to use animal models such as rodents. Specifically for hallucal grasping, mice raised in enclosures with complex simulated fine-branch arboreal substrates have been observed to habitually use their hallux in grasping bouts to aid in above branch balance (Byron et al., 2011). These same mice have Mt1s with diaphyses that are relatively more robust (as determined from cross-sectional geometric properties) than those mice raised on the ground that do not use their hallux to grasp the substrate (Byron et al., 2015). These studies highlight how habitually different locomotor behaviors and substrate use during development can influence the relative strength of the Mt1. Moreover, it provides additional support for the hypothesis that behavior (in this case, hallucal grasping) influences habitual loading, which in turn influences bone cross-sectional shape. For primates, however, an approach examining a cross-sectional ontogenetic sample of taxa with different developmental patterns in habitual hallux use is more feasible than longitudinal lab-based experiments (but see Jungers and Fleagle, 1980; Young et al., 2010; Young and Heard-Booth, 2016).

The cheridia of young non-human primates are structured for increased grasping ability (Young and Heard-Booth, 2016). During the earliest months or even the first few years of life, infant and smaller juvenile primates rely on their mothers for survival including traveling long distances (e.g., Fragaszy et al., 1989; Altmann, 2001; Ross, 2001). The mode in which they are carried by their mothers can influence the grasping strategies used by the hands and feet. In both Old World monkeys and African apes, mothers initially carry their small infants ventrally on their bellies (Nakamichi and Yamada, 2009). During ventral carriage, the infant must overcome gravitational forces, as well as all oscillatory forces caused by the mother’s locomotion, that are tending to dislodge it. Relatively large grasping hands and feet in some infant primates can facilitate their ability to cling to their mother’s belly (e.g., Grand, 1977; Jungers and Fleagle, 1980; Raichlen, 2005; Young and Heard-Booth, 2016).

As they grow, many young primates eventually shift to a more dorsal carriage position on their mother’s lower back or thorax (Nakamichi and Yamada, 2009; Anvari et al., 2014). In a dorsal position, manual and pedal grasping may not be as vital for surviving a long bumpy ride when the mother is walking quadrupedally, but they likely are still being used to some extent when she is climbing or engaged in acrobatic arboreal activities like suspension. After

reaching a certain body size or mechanical competency, young juveniles become locomotor independent. The timing of locomotor independence has been shown previously to correspond well with clear changes in limb bone rigidity, strength, and shape properties in both monkeys and apes (Ruff, 2003b; Young et al., 2010; Russo and Young, 2011; Sarringhaus et al., 2016). Limb bones of very young individuals are overly built (relative to body mass and/or bone length) and decrease in structural competency (i.e., safety factors) as they grow and become more proficient in their movements (Ruff, 2003b; Young et al., 2010). In the case of the hallux, it too may be biomechanically stronger than its needs to be in very young individuals because it is used heavily to grasp their mothers during ventral carriage. As primates become locomotor independent, the relative strength of their Mt1 may also decrease if they graduate to using their hallux with relatively less force. That would be the case for many monkeys and apes that may rely less on their grasping feet after infancy, but for others that continue to rely heavily on them throughout life, it may not.

The gradual (or abrupt) changes in habitual substrate use and preferred locomotor and postural modes during development may also change the nature in which the hallux is used in grasping during an individual's lifetime. Locomotor behaviors in African apes are more variable early on in life, where younger chimpanzees and gorillas are not only quadrupedal, but also engage in more forelimb suspension, vertical climbing, bipedalism and other behaviors (e.g., Doran, 1992, 1997; Sarringhaus et al., 2014). Additionally, African apes tend to become less arboreal with age, thereby reducing their reliance on forelimb suspensory and vertical climbing bouts (Doran, 1992, 1997; Sarringhaus et al., 2016). As African apes continue to use terrestrial substrates more with age, their increased reliance on quadrupedalism and simultaneous reduction in vertical climbing activity may result in a lower frequency of powerful hallucal grasping later in ontogeny. In contrast, many monkeys like rhesus macaques primarily engage in arboreal quadrupedal walking upon reaching locomotor independence, with other behaviors like running, leaping and climbing are used to a lesser degree throughout ontogeny and into adulthood (Rawlins, 1982; Wells and Turnquist, 2001). Therefore, it is likely that growing monkeys may also be power grasping with their hallux only very early in life, and that the use of the hallux and the mechanical stresses it is subjected to into adulthood become less forceful and less variable over time in both direction and magnitude. When comparing monkeys to African apes, however, since the former are more arboreal throughout ontogeny and into adulthood, it is possible that older monkeys will have a biomechanically more robust Mt1 than older apes, assuming that they actually engage their hallux for frequent bouts of powerful hallucal grasping.

In this study, we test the hypothesis that ontogenetic changes in locomotor and postural behaviors can alter the form and function of the developing Mt1, specifically its midshaft robusticity and shape. Additionally, we test the hypothesis that different patterns in locomotor ontogeny between apes and monkeys will produce different patterns of Mt1 midshaft strength and shape development in both groups. Three predictions are made: 1) Mt1 robusticity will be relatively greater at younger ages in both apes and monkeys; 2) Mt1 robusticity will be relatively larger in monkeys compared to apes, especially at older ages; and 3) Mt1 midshaft shape will see greater changes in apes than monkeys across ontogeny. Here we use the rhesus macaque (*Macaca mulatta*) and common chimpanzee (*Pan troglodytes*) as representative monkey and ape species, respectively. Both are ideal

comparative taxa for this cross-sectional ontogenetic analysis because much is known about their life histories and ontogenetic changes in locomotor and positional behavior (Rawlins, 1982; Doran, 1992, 1997; Wells and Turnquist, 2001; Sarringhaus et at., 2014, 2016).

Materials and Methods

All five metatarsals were analyzed from a cross-sectional ontogenetic sample of 73 rhesus macaques (*Macaca mulatta*) and 79 common chimpanzees (*Pan troglodytes*). The sample of macaques was derived entirely from the skeletal collection in the Laboratory of Primate Morphology and Genetics of the Caribbean Primate Research Center (CPRC), located at the University of Puerto Rico. This collection contains a large number of complete skeletons at all developmental stages from a colony of free-ranging monkeys that were reared in a uniform environment and that have been extremely well-documented from long term observation (e.g., Rawlins and Kessler, 1986; see also literature cited in Dunbar, 2012). Multiple museums were needed for the chimpanzee sample to obtain sufficient sample sizes across all developmental age groups. The sample of wild-shot chimpanzees come from the collections at the: 1) Anthropologisches Institut und Museum (AIM) of the Universität Zürich, Zürich, Switzerland; 2) the Royal Museum for Central Africa (RMCA) in Tervuren, Belgium; 3) the National Museum of Natural History (NMNH) in Paris, France; and 4) the Hamann-Todd Collection at the Cleveland Museum of Natural History (CMNH).

Because actual ages of the chimpanzee specimens were not known, five developmental age class categories (Table 1) were adopted based on dental eruption schedules described in Dean and Wood (1981), an approach also used by Sarringhaus et al. (2016). The rhesus macaques at the CPRC all have documented ages at death, but dental eruption stages for these specimens were assessed following Kenney (1975) in order to make appropriate comparisons of the macaques with the chimpanzees across developmental stages. According to Cheverud (1981), dental eruption stages follow a similar order of eruption timing in both rhesus macaques and chimpanzees. For both species, age Group 1 are young infants that consists of individuals that rely on their mothers (or other caregivers) to facilitate locomotion across long distances and age Group 2 are older infants and young juveniles who are becoming locomotor independent (i.e., transitional locomotion) (Doran, 1997; Wells and Turnquist, 2001). Age Groups 3 and 4 are older juveniles and adolescents individuals who are locomotor independent, and are increasing in somatic growth, while age Group 5 individuals are full adults in all aspects of form and behavior. Metatarsal epiphyses begin to fuse between three and four years of age in rhesus macaques (Bourne, 1975), thus corresponding to age Group 3 in this study. Age Groups 4 and 5 macaques visually appeared to have fully fused metatarals. Similarly, metatarsal epiphyses are partially fused between eight and nine years of age in chimpanzees (Brimacombe et al., 2015), also corresponding to age Group 3 in this study. Age Group 4 and 5 chimpanzees all appeared to have fused metatarals upon visual inspection. Table 2 provides sample sizes for each species within each age group.

Physical or digital cross sections of long bones are ideal to quantify cross-sectional geometric variables, especially of small bones like metatarsals. Unfortunately, physically sectioning museums specimens is destructive and often prohibited, and access to computed

tomography (CT) or μCT facilities were not available at the time when a portion of the data analyzed here were collected (Dunsworth, 2006). In the absence of CT scans, bi-planar radiography combined with latex molding (i.e., latex cast method; LCM) of the external surface serves as an adequate substitute because it can approximate true section properties of bone (e.g., Stock, 2002; O'Neill and Ruff, 2004; Marchi, 2005). Moreover, combining long bone cross-sectional geometry data acquired from multiple methods (i.e., CT and biplanar radiography) is not uncommon since there are likely no systematic differences (Polk et al., 2000). All chimpanzees in age Groups 2–5, and a single individual in Group 1, were analyzed using the LCM. Macaques from age Groups 3 and 4 were also analyzed using the LCM. Group 1 chimpanzees, and macaques from Groups 1, 2 and 5 were analyzed from CT or μCT scans.

The LCM for reconstructing bone cross sections combines bi-planar radiography with latex molding of the external surface of the diaphysis. In the LCM sample, midshaft was determined as the midpoint of absolute bone length. To assess the circumference of the outer diaphyseal surface in cross section, silicone-based molds of the metatarsal midshafts were photographed with a digital camera and measurements were made using ImageJ software (Rasband, 1997–2016). To reconstruct the circumference of the medullary cavity, thickness of the medial, lateral, dorsal, and plantar cortices were measured using ImageJ from two radiographs of each metatarsal taken in the dorsal-plantar and the medio-lateral planes, corrected for parallax, and then drawn inside the scaled digital photograph of the mold of the outer circumference. Metatarsal anatomical orientations followed Marchi (2005). These four cortical thickness lines help determine the size and placement of an ellipse drawn in the center of the section to approximate the medullary cavity. Cross-sectional properties were obtained from these reconstructed images of the midshaft cross sections with the MOI (Moment of Inertia) script (written by Timothy Ryan) in the software IDL (Interactive Data Language; RSI®). A more detailed description of the LCM methodology employed here, including equipment used, error studies, and parallax correction can be found in Dunsworth (2006).

Computed tomography scans of age Group 1 chimpanzees come from two sources. Four individuals were scanned in the UZ Leuven Department of Radiology (Leuven, Belgium) using a Siemens CT-SOM5 SPI medical scanner. The remaining individuals were scanned in the Department of Radiology of the Pitié-Salpêtrière Hospital (Paris, France) using a Philips iCT256 medical scanner. Similar scanning parameters were used in both facilities: energy: 140 kVp; current: 130–253 mA; slice thickness: 0.67 mm; reconstruction increment: 0.3 mm. The raw data were reconstructed as 16-bit DICOM images using a bone reconstruction algorithm (i.e., a "sharp" kernel). The CT data from both sources were analysed using Avizo Lite v. 9.0 software following the protocol outlined in Jashashvili et al. (2015) and Dowdeswell et al., (in press), which involved isolating individual metatarsals (since multiples bones were scanned simultaneously), 3D re-orienting of each bone into a standardized anatomical position (following Marchi, 2005), extracting the re-oriented slice corresponding to midshaft from its inter-articular length. The midshaft slices were imported into ImageJ where it was measured using the Slice Geometry protocol and default single slice thresholding option in the BoneJ plugin (Doube et al., 2010).

For the macaques in age Groups 1, 2 and 5, μCT scanner technology was used to acquire digital cross section. The Group 5 macaques were scanned at the University of Southern California's Molecular Imaging Center using a SCANCO Medical 50 specimen scanner with a voxel resolution of 48.4 μm. Scanning parameters included: energy: 90 kVp; current: 144 μA; filter: Al 0.5 mm; integration time: 100 ms; projections: 750/180°; image size: 1024×1024 pixels. The raw data were reconstructed as 16-bit DICOM images and then converted to 8-bit DICOM images for analysis. The image stack for each metatarsal was imported into ImageJ software where it was first re-oriented using the Moment of Inertia protocol in the BoneJ plugin for ImageJ software. This plugin calculates the three orthogonal principal axes (x, y, z) from the raw pixel data after thresholding for bone pixels in the entire stack and produces a new image stack that is standardized in orientation (i.e., rotation and translation). The same anatomical definitions for the bi-planar radiography and CT methods described above were implemented here as well (following Marchi, 2005). After identifying the reoriented slice corresponding for midshaft (based on inter-articular length), the Slice Geometry protocol in BoneJ was used to calculate the cross-sectional geometry variables using the default single slice thresholding option.

The age Group 1 and 2 macaques were scanned at The Pennsylvania State University's Center for Quantitative using a OMNI-X HD600 Industrial microCT scanner and X-TEK microfocus subsystem (Varian, Inc) with a voxel resolution of 10.55 μm. Scanning parameters included: energy: 180 kVp; current: 0.11 mA; projections: 2400/180°; image size: 1024×1024 pixels. Prior to scanning, the five metatarsals for each individual were set up in a standardized anatomical position (following Marchi, 2005) so they could be scanned simultaneously. For this sample, only the midshaft regions were scanned to save on time and cost, and the data were saved as 8-bit TIF images. The single slices corresponding to midshaft (based on bone length) were imported into ImageJ for analyzis with the MomentMacro plugin (http://www.hopkinsmedicine.org/fae/mmacro.html) using the default thresholding option native to ImageJ.

Metatarsal strength and robusticity can be estimated in many ways from its cross-sectional geometry including calculations of cortical area and section modulus (Marchi, 2005; Griffin and Richmond, 2005; Jashashvili et al., 2015). In this study, we emphasized the polar second moment of area (*J*), which is a measure of twice bending rigidity as well as torsional rigidity, and is calculated by adding together the maximum and minimum second moments of area, *Imax* and *Imin*, respectively, which are measures of bending rigidity (e.g., Ruff and Hayes, 1983). Following the conclusions put forth by Lieberman and colleagues (2004) regarding interpretation of cross-sectional geometric variables, there were three primary reasons why *J* was emphasized over other variables. First, it is not entirely clear in what direction (e.g., mediolateral; dorsoplantar) or by what nature (e.g., compression, bending or torsion) the metatarsals are loaded when used during locomotion or other behaviors with pedal grasping. It is likely that they are experiencing multiple external forces and from multiple directions (e.g., Preuschoft, 1970), and *J* can cautiously account for these. Second, it has been shown that *J* is a reliable predictor, although not without error, of average bending rigidity when experimental data of bone loading is unavailable (Ruff, 2002; Organ, 2010). Third, it is a variable that can be compared across datasets that use different data acquisition protocols (Polk et al., 2000; O'Neill and Ruff, 2004) as was necessary in this study (see above).

To compare metatarsal rigidity values across age groups that differ in size and absolute length (L), as well as between macaques and chimpanzees (with the latter being significantly larger in mass [Smith and Jungers, 1997]), dimensionless scaled J (= J_s) values were calculated as $J^{0.25}/L$. It is important to note that conventionally J is scaled by the product of L and body mass (Polk et al., 2000; Ruff, 2000), however, in this study only L was used because actual body mass data for most of the sample was not available (cf. Organ, 2010)[1], and it seemed illogical to estimate body mass from femoral head measurements since extrapolating these data for infants/juveniles from adult-derived equations (e.g., Ruff, 2003a) would only introduce more sources of error in the analyses. Moreover, fusion of the femoral head does not begin until about three years of age in rhesus macaques (Bourne, 1975) and 10 years of age in chimpanzees (Zihlman et al., 2007) which correspond to age Group 3 individuals in this study, thus making measurements of femoral heads prone to error. Length values were obtained either with digital calipers on actual specimens or from virtual 3D surface renderings of the bones derived from computed tomography (CT) scans. For chimpanzee infants and young juveniles with unfused epiphyses, the epiphysis was placed on the end before measuring length and if the epiphysis was not present, the length of the epiphysis was estimated using specimens of similar age, size, and sex. Bone length for infant and young juvenile macaques with unfused epiphyses was measured withouth re-attaching the epiphyses because they were usually missing in the collections. Moreover, the epiphyseal length was not estimated in these specimens given the possibility of introducing error given the very small size of these boney elements (<1.0 mm).

Because younger individuals will have shorter metatarsals, and smaller bones tend to have smaller J values (e.g., Ruff, 2000), we also assessed changes in metatarsal rigidity across ontogeny by evaluating whether J scales isometrically or allometrically with L for each digit in both species. To accomplish this, the natural log (ln) of L was regressed against ln J using reduced major axis (RMA) regression techniques to calculate slope and its 95% confidence intervals (CI). A slope that was not significantly different from 4.0 (i.e., was within the 95% CI of the slope) was considered isometric. Slopes significantly lower than 4.0 were considered to display negative allometry. Slopes significantly greater than 4.0 were considered to display positive allometry. Past v.3.04 software (Hammer, 2014) was used to perform the RMA regression analyses.

A ratio of *Imax* and *Imin* values for only the Mt1 were also used to calculate its midshaft shape. A number of studies have argued that an *Imax/Imin* ratio can be used as a proxy for inferring whether a long bone experiences loads that are relatively complex rather than uniform in direction (e.g., Carlson, 2005, Carlson and Judex, 2007; Patel et al., 2013; Sarringhaus et al., 2016). Values greater than 1.0 indicate an elliptical cross-sectional shape and suggests that a bone experiences more habitual or uni-directional loading. The greater deviation from 1.0 would further suggest a loading environment that was relatively more uniform.

[1]Alternatives for body mass, such as femoral head bread (*FHB*) can be used and thus J could be scaled by the product of L and *FHB* (e.g., Dunsworth, 2006). This approach, however, was not followed here because FHBs for Age Group 1 chimpanzees were unavailable. We did test this approach in the macaque sample (since we had estimates of *FHB*s for all individuals) and found near identical patterns when J is scaled by L or when J is scaled by Lx*FHB* (see Figure S1 in Supplemental Online Material, SOM). A likely reason for the similarities in both scaling approaches is because macaque L and *FHB* scale isometrically (see Table S1 in SOM).

Finally, to assess the robusticity of the Mt1 compared to the other metatarsals (Mt2–5) over ontogeny, a ratio was created of relative Mt1 J_s values (= J_{SRel}). This was accomplished by dividing Mt1 J_s by the geometric mean of Mt2–5 J_s values,

$$J_{SRel} = \mathrm{Mt1}\ J_s / (\mathrm{Mt2}\ J_s \times \mathrm{Mt3}\ J_s \times \mathrm{Mt4}\ J_s \times \mathrm{Mt5}\ J_s)^{0.25}$$

A J_{SRel} value greater than 1.0 indicates that Mt1 J_s is greater than Mt2–5 J_s.

The J_s for each metatarsal, and J_{SRel} and *Imax/Imin* ratios for only the Mt1s, were compared across age groups within macaques and chimpanzees. Additionally, J_s and J_{SRel} values for each metatarsal were compared between macaques and chimpanzees within each age group. Comparisons between age groups or species were made with ANOVAs, and if significant, post-hoc comparisons were made using Tukey's HSD tests. These statistical analyses were performed in JMP v.12 software (SAS Institute, Inc.).

Results

Descriptive statistics for *L*, *J*, and J_s for each age group of both species are presented in Table 2. The Mt1s of younger macaques in age Groups 1 and 2 have significantly larger J_s values than that of their older counterparts in age Groups 3–5 (Tables 2 and 3; Fig. 1). The same pattern of decreased rigidity over ontogeny is seen in chimpanzees, although differences are only significant in age Group 1 vs other older age groups (Table 2). As macaques and chimpanzees continue to grow after becoming locomotor independent and into adulthood, the relative rigidity of their Mt1s remains low, but begin to become slightly stronger in to age Group 5. In the macaque sample, J_s for Mt1s are lowest in age Group 3, whereas in chimpanzees they are lowest in age Group 4 individuals (Table 2; Fig. 1). However, there are no significant differences across age Groups 3–5 in either species.

In macaques, J_s for Mt2–5 changes over ontogeny (Tables 2 and 3, Fig. 1). Except for Mt2, age Group 1 individuals have more rigid lesser metatarsals than age Group 2 individuals. Younger macaques in age Groups 1 and 2 also have significantly more rigid Mt2–5s than older individuals in age Groups 3–5. Generally, there are few significant differences in $_s$ between the three older macaque groups. As seen in Mt1, J_s for Mt2–5 appear to be the lowest in age Group 3 individuals (Fig. 1).

In chimpanzees, J_s for Mt2–5 are in general not significantly different across age groups (Tables 2 and 3, Fig. 1). However, there are two notable exceptions. First, the Mt5 of age Group 1 chimpanzees is structurally the most rigid with a significantly higher $_s$ than all older individuals. Second, the Mt2 of age Group 5 chimpanzees is significantly more rigid with higher J_s values than all younger individuals.

Across age groups, Mt1 J_s is always significantly greater in chimpanzees than in macaques, and these differences are greatest in older individuals in age Groups 3–5 (Tables 2 and 4). Similarly, chimpanzees in age Groups 3–5 have Mt2–5s with a significantly larger J_s when compared to macaques of the same relative age (Table 4). In general, chimpanzees and macaques in age Groups 1 and 2 do not significantly differ from each other in J_s values for

Mt2–5. The one exception is that macaques have significantly more rigid Mt2s in individuals that make up age Group 1 (Table 4).

Older individuals of both species have longer metatarsals and larger *J* values. However, the scaling between *J* and *L* differs between macaque and chimpanzees (Table 5). In macaques, metatarsal *J* and *L* scale significantly with negative allometry for all metatarsals (mean slope = 2.65). In chimpanzees, Mt1, Mt4 and Mt5 *J* and *L* scale with significant negative allometry (mean slope = 3.42), while in the Mt2 they scale with significant positive allometry (slope = 4.51). Although *J* and *L* in the chimpanzee Mt3 do not scale significantly different from isometry and is within the 95% CI of 4.0 (upper bound of slope = 4.0044), this is effectively negative allometric (with a calculated slope = 3.81). Collectively, RMA slope values for the macaques are significantly lower across all metatarsals indicating that the reduction in rigidity as metatarsals get longer over ontogeny is greater, a pattern that supports the trends noted above for J_s over ontogeny (Fig. 1). In both macaques and chimpanzees, the RMA slopes for the Mt1 is always smaller than the RMA slopes for Mt2–5 (Table 5).

In both macaques and chimpanzees, Mt1 J_{SRel} is always greater than 1.0 indicating that the Mt1 is relatively stronger than Mt2–5 at any age (Table 6, Fig. 2). Also in both taxa, $_{SRel}$ is greatest in age Group 1 individuals, although this is only statistically significant in chimpanzees (Tables 6 and 7). Across age Groups 2–5, J_{SRel} decreases in chimpanzees (although not significantly) while remaining comparatively constant in macaques (Tables 6 and 7; Fig. 2). Chimpanzees also have significantly higher J_{SRel} values for each ontogenetic age group except age Group 3 (Table 8).

Both macaques and chimpanzees have Mt1s that are elliptical in shape with *Imax*/*Imin* ratios always greater than 1.0. Also, in general, macaques have more elliptical cross sections than chimpanzees in all age groups (Table 9; Fig. 3). Over ontogeny, Mt1 shape significantly changes in macaques to become even more elliptical where age Groups 1 and 2 have a mean shape value of 1.37 and adults in age Groups 4 and 5 have mean shape values of 1.51 (Tables 9 and 10, Fig. 3). In contrast Mt1 shape does not significantly change in chimpanzees over ontogeny (Table 10).

Discussion

The timing of locomotor independence along with changes in habitual locomotor behaviors and substrates used throughout ontogeny can influence how primates use their hallux as a grasping organ. Accordingly, there should be accompanying changes in foot bone structural properties during ontogeny that reflect changes in grasping performance (i.e., force production and frequency of use), especially in the hallucal metatarsal (Mt1). The primary aim of this study was to test this hypothesis by evaluating metatarsal midshaft rigidity, estimated from the polar second moment of area (*J*), and metatarsal midshaft cross-sectional shape, calculated from the ratio of maximum and minimum second moments of area (*Imax*/*Imin*), in a cross-sectional ontogenetic sample of common chimpanzees and rhesus macaques, two taxa with different positional behaviors, substrate preferences and foot use across ontogeny.

As predicted, the Mt1 of both species is more rigid (relative to length) in younger individuals, and relative rigidity gradually decreases with age in both species (Fig. 1; Table 2). This lends support for the hypothesis that the youngest macaques and chimpanzees use their hallux with relatively greater force during pedal grasping. As individuals of each species age, grow, become locomotor independent, and gradually obtain a habitual repertoire of positional behaviors and substrate preferences, their Mt1 becomes relatively less rigid, with no noteworthy differences in robusticity after maturing to age Group 3. Studies of primate life history events have shown that different primates achieve locomotor independence at different absolute ages. Although young African apes can begin to locomote after three months of age, they do so in near proximity to their mothers and on average, chimpanzees and gorillas are completely locomotor independent of their mothers by four or five years of age, respectively (Doran, 1997). In contrast, more precocial monkeys like baboons are independent of their mothers as early as three months of age and completely by 8–12 months (Altman, 2001; Altman and Samuel, 1992; Rawlins, 1982). In rhesus macaques, locomotor independence is complete by 18 months of age (Wells and Turnquist, 2001). Despite these absolute age differences in African apes and monkeys, this transition period of locomotor independence corresponds to the same dental development age (here identified as age Group 2; see Table 1), and it is during this stage where relative Mt1 rigidity begins to significantly drop, while still remaining higher than that of individuals in age Group 3.

In macaques, relative weakening in Mt2–5 bone rigidity is also observed over ontogeny, although the drop in relative Mt1 rigidity is much greater than in the lesser toes. It is worthwhile to note, however, that age Group 3 macaques consistently have the lowest J_S values (Fig. 1), but the differences are not significant when compared to older age Group 4–5 animals (Table 3). Metatarsal epiphyses begin to fuse in macaques around four years of age (Bourne, 1975) which coincides with age Group 3 in this study, and thus this may be the reason for the relatively lowest values at this time. Increase in relative rigidity in age Groups 4–5, although not significant, may be related to the fact that metatarsals a nearly fused and almost done growing. In contrast, chimpanzee lateral metatarsals do not show a consistent pattern of relative loss in rigidity. Rather, the Mt2–5s of age Group 5 chimpanzees tend to be relatively more rigid than age Groups 3 and 4 animals. Specifically, age Group 4 individuals consistently have the lowest J_S values (Fig. 1) with significant differences from older age Group 5 individuals occurring in Mt2–4 (Table 3). It is unlikely that this difference is related to smaller samples sizes of age Group 4 chimpanzees compared to other age groups (Table 2). Additionally, this difference in chimpanzees is not likely related to any specific ontogenetic changes in locomotor behaviors since the animals in these age groups are predominantly quadrupedal and have already reduced their use of suspensory or vertical climbing behaviors (Doran, 1997; Sarringhaus et al., 2014; 2016). It is possible, however, that with increased somatic growth into age Group 5 coupled with the frequent use of terrestrial substrates (e.g., Doran, 1997; Sarringhaus et al., 2016) that the middle part of the foot becomes slightly more rigid to withstand relatively high ground reaction forces during ground walking and galloping (Demes et al., 1994), as well as when using variable foot postures and kinematics during terrestrial locomotion (e.g., Vereecke et al., 2003). In general, however, we think it prudent to say that robusticity measures do not profoundly

differ between individuals within age Groups 3, 4, and 5 for any of the metatarsals in either species except the Mt2 of chimpanzees (see below for further discussion).

It is evident when comparing relative rigidity of the Mt1 with that of the other metatarsals (i.e., J_{SRel}) that the hallucal metatarsal is always significantly more rigid in both rhesus macaque and chimpanzee feet (Table 6; Fig. 2). By in large, this pattern also holds when comparing absolute J values across digits within species (Table 2). Additionally, the Mt1 remains relatively more rigid than Mt2–5 throughout ontogeny in both groups, and the adult patterns reported here for both macaques and chimpanzees are consistent with previous studies on adult great ape (Marchi, 2005) and human (Griffin and Richmond, 2005) metatarsal cross-sectional geometry (i.e., the Mt1 has the strongest and most rigid midshaft). It is important to note, however, that Mt1 J_{SRel} has a different ontogenetic pattern within macaques versus within chimpanzees. In macaques the magnitude of difference does not significantly change as animals age and grow, except for an unusual significant difference between age Group 1 and 2 versus age Group 4 individuals (Tables 6 and 7). Unfortunately, it is not possible to conclude why this significant different exists at this time and speculation is not warranted. Therefore, not only is the macaque Mt1 absolutely and relatively more rigid than the other metatarsals across all age groups, this magnitude of difference between hallucal rigidity and that of the other metatarsals does not significantly change with age. In contrast, within chimpanzees J_{SRel} is significantly greater in age Group 1 individuals compared to older animals (Tables 6 and 7) thereby effectively demonstrating that the Mt1 is "hyper-robust" in the youngest animals. Although the Mt1 of age Group 1 chimpanzees are absolutely the shortest (Table 2), their "hyper-robust" appearance is not simply a phenomenon of scaling (i.e., small denominator). That is because Mt1 length relative to Mt2–5 lengths is the same across chimpanzee ontogeny (see Figure S2 in the SOM). In contrast, Mt1 length relative to Mt2–5 lengths decreases over ontogeny in rhesus macaques. Moreover, Mt1 J_{SRel} is significantly larger in chimpanzees than in macaques for both young and old animals (Table 8). These findings demonstrate that while forces acting on the hallux are relatively larger than in the other metatarsals at all ages, powerful hallucal grasping is likely more routinely used in chimpanzees than in macaques at the youngest ages.

As documented by other researchers, the timing of locomotor independence corresponds with distinct changes in limb bone strength and shape properties in both monkeys and apes (Ruff, 2003b; Young et al., 2010; Russo and Young, 2011; Sarringhaus et al., 2016). Limb bones of very young individuals are overly built (relative to body mass and/or bone length) and decrease in structural competency (i.e., safety factors) as they grow and become more proficient in their movements (Ruff, 2003b; Young et al., 2010). In the case of the hallucal metatarsal, it too appears to be overly built or hyper-robust in the youngest individuals of both species (Fig. 1) and J has a negative allometric relationship with metatarsal length (Table 5), possibly because they are heavily used in pedal grasping early on in life when they need to hold on to their mothers while being carried. As both chimpanzees and monkeys transition to become locomotor independent, the relative rigidity of their Mt1 decreases since they probably use their hallux with relatively less force. The fact that the Mt1, along with more proximal bones in the upper and lower limbs, are relatively stronger in younger versus older individuals further emphasizes that this is a general developmental phenomenon

in both primates (Ruff, 2003b; Young et al., 2010; Russo and Young, 2011; Sarringhaus et al., 2016) and other mammals (Carrier, 1983; Main and Biewener, 2007).

Like the Mt1, *J* values for Mt2–5 of macaques also scale with negative allometry with metatarsal lengthening. And in chimpanzees, the Mt4 and Mt5 also scale with negative allometry, whereas Mt3 scales isometrically. In these cases (albeit to a lesser degree in the chimpanzee Mt3), the foot bones are relatively less robust in older individuals with longer metatarsals. The one notable exception to this general pattern is in the chimpanzee Mt2 where *J* scales with significant positive allometry with length during growth (Fig. 1; Table 5). Thus, older chimpanzees have significantly stronger second metatarsals for their given length. This unusual pattern is likely related to the fact that the medial column of metatarsals (especially the Mt2) experiences higher plantar pressures per unit time (i.e., pressure impulses) compared to the lateral column (Mt4 and Mt5), especially when chimpanzees engage in vertical climbing and arboreal quadrupedal locomotion (Wunderlich and Ischinger, 2017). Thus, the medial side of the foot needs to be structurally stronger than the lateral side. Patterns of plantar pressure in the macaque foot (Higurashi et al., 2010; Hirasaki et al., 2010) suggest that the lateral metatarsal column (Mt4 and Mt5) is loaded more, but these patterns are highly variable with no one side (i.e., medial or lateral metatarsal column) being loaded consistently within and between arboreal and terrestrial steps, thus possibly explaining why *J* in no one metatarsal scales differently with length compared to the others.

The Mt1s of the youngest macaques and chimpanzees have elliptical cross-sectional shapes with *Imax*/*Imin* ratios greater than 1.0 (Table 9). It is believed that a loading environment that is relatively uniform in direction will cause bones to be more elliptical, whereas more variable (i.e., multi-directional) loads causes bones to adapt more circular shapes (e.g., Carlson, 2005, Carlson and Judex, 2007; Patel et al., 2013; Sarringhaus et al., 2016). Because even the youngest macaques and chimpanzees already have elliptical Mt1s, this implies that there is some baseline genetic component dictating its shape (and ultimately its rigidity and strength) and that the magnitude and direction of mechanical loads is not the only determinant of bone cross-sectional shape (e.g., Jepsen et al., 2007; Wallace et al., 2012; Burr and Organ, 2017). It would be worthwhile to determine what Mt1 cross-sectional shape looks like in either a late-term fetus or a newborn, a period of life when the mechanical loads that the hallux is exposed to would be expected to be smaller in magnitude and less uniform in direction. Postnatally, the hallux is ultimately loaded in compression, bending, and torsion and any changes in cross-sectional shape are likely influenced by its loading environment (Jashashvili et al., 2015). As macaques age, the cross-sectional shape of the Mt1 becomes significantly more elliptical (Table 10), indicating that mechanical loads acting on the Mt1 become relatively more uniform in direction as macaques get older. This finding is counter what was predicted above and would suggest that as macaques grow and become both locomotor independent and competent, their use of diverse hallucal postures (including strong bouts of grasping) becomes less frequent despite habitually using arboreal substrates (Wells and Turnquist, 2001). Although EMG data from the flexors of the hallux have not been studied in rheses macaques during arboreal locomotion, these muscles have been shown to be only minimally active in regular bouts of wide and narrow pole quadrupedalism in captive capuchin monkeys (Patel et al., 2015a). Assuming quadrupedal foot postures and muscle recruitment patterns are constant across similar-sized monkeys on

arboreal supports, then it is also probable that forceful contractions of these same muscles in rhesus macaques may be infrequent, further indicating that powerful hallucal grasping is a relatively rare occurance (i.e., is more postural than locomotor) during stable bouts of movement.

In contrast, and again counter to predictions outlined above, as chimpanzees age, the cross-sectional shape of their Mt1 does not become significantly more or less elliptical (Tables 9 and 10). This suggests that the direction of loads acting on the chimpanzee hallux is variable throughout ontogeny despite the fact that older chimpanzees are less arboreal than younger ones (Doran, 1997; Sarringhaus, 2014, 2016). Moreover, because Mt1 cross-sectional shape of chimpanzees is less elliptical than macaques across all ages, it indicates that the chimpanzee hallux is used more varyingly in both grasping when in the trees and supporting body weight in a strut-like fashion when on the ground, and is well adapted mechanically to be used on a variety of substrate types (e.g., arboreal vs. terrestrial) and orientations (e.g., horizontal vs. oblique vs. vertical) (e.g., Patel et al., 2017; Wunderlich and Ischinger, 2017).

At the youngest developmental ages, relative rigidity of Mt2–5 is not significantly different between macaques and chimpanzees. In contrast, relative rigidity is significantly greater in the chimpanzee Mt1 at the youngest ages (Tables 2 and 4; Figs. 1). As both species mature past age Group 2, the differences in macaque and chimpanzee Mt2–5 relative rigidity/robusticity becomes significant, with the latter having relatively more rigid metatarsals. Moreover, this difference between two species is even more prominent in the hallucal metatarsal where the Mt1 is significantly stronger in the chimpanzee in older individuals. These observed differences in Mt1 strength between macaques and chimpanzees across all stages of development counters the predicted form-function relationship related to hallucal grasping ontogeny discussed above. Rather, these data provide evidence demonstrating that chimpanzees in general have biomechanically more robust hallucal metatarsals than macaques at all stages of growth. Because chimpanzee Mt1s are absolutely and relatively longer than macaque Mt1s (Table 2 and Fig. S2), the greater ridgidity in the former is not due to scaling by length alone (Table 8). While the reasons for this finding are likely complex, one possibility is that chimpanzees may need to have stronger metatarsals, especially the Mt1, into adulthood because they spend more time on less compliant terrestrial subtrates (Doran, 1992; 1997). An ontogenetic study of other terrestrial primates such as baboons and gorillas could help test this hypothesis. Another reason could be that the chimpanzee hallux experiences relatively large forces during vertical climbing (Wunderlich and Ischinger, 2017) which is a behavior used at all ontogenetic stages, although much less in older adults (Sarringhaus et al., 2014).

Another hypothesis is that differences between macaques and chimpanzees also represent a general monkey versus ape (i.e., phylogenetic) pattern that has been previously noted based on external morphology alone (e.g., apes having relatively larger Mt1s; Conroy and Rose, 1983; Wunderlich, 1999; Patel et al., 2017) and would be consistent with known behavioral differences in foot function and use in these two groups. Additional cross-sectional geometry data from a phylogenetically diverse sample of ape and monkey species, however, would be needed to endorse this hypothesis. Because of the varying body sizes within and between monkey and ape species (Smith and Jungers, 1997), such analyses could also

benefit from incorporating proper body mass estimates (i.e., not specifically FHBs as noted above) when scaling rigidity measures such as *J* (e.g., Polk et al., 2000). If this is eventually confirmed, it could provide the comparative biomechanical context needed to evaluate the behavior and pedal function of the earliest apes like *Proconsul/Ekembo* and to see if they had hallucal grasping strategies (or terrestrial and climbing positional behaviors) more like extant great apes or like extant monkeys (Conroy and Rose, 1983; Dunsworth, 2006; Patel et al., 2017). This would provide an important evolutionary context to some of the major morphological and behavioral differences that we see today in the feet of apes and monkeys.

In conclusion, different patterns of development in metatarsal diaphyseal ridgidity and shape appears to reflect real differences in which the foot, and in particular the hallux, functions across ontogeny in both apes and monkeys.

Supplementary Material

Refer to Web version on PubMed Central for supplementary material.

Acknowledgments

We would like to thank the following people and institutions who let us study chimpanzee specimens in their collections: Marcel Zefferer and Frau Müller of the Anthropological Institute und Museum of the Universität Zürich; Emmanuel Gilissen, Wim Wendelen, Wim van Neer, and Willem van Hoef of the Royal Museum for Central Africa and the Gasthuisberg Hospital; Christine Lefèvre of the National Museum of Natural History in Paris; Lyman Jellema of the Hamann-Todd Collection at the Cleveland Museum of Natural History. We also greatly appreciate the assistance from Terry Kensler and the Laboratory for Primate Morphology and Genetics of the Caribbean Primate Research Center for providing access to rhesus macaque specimens in their care. The Caribbean Primate Research Center receives funding from the National Institutes of Health (NIH 8 P40 OD012217-25).

MicroCT scanning at the University of Southern California's Molecular Imaging Center was facilitated by Tautis Skorka and Grant Dagliyan. Assistance with microCT scanning at The Pennsylvania State University's Center for Quantitative Imaging was provided by Timothy Ryan. We are very thankful to Philippe Grenier and Bettina Begenau of the Hôpital Pitié Salpêtrière and Walter Coudyzer of UZ Leuven for facilitating use of their CT scanners. Additionally, we thank the Evolutionary Studies Institute at the University of the Witswatersrand for access to their VIP computing laboratory for data analysis.

Funding for this research was provided by the National Science Foundation (BCS # 1317047 [to BAP]), The L.S.B. Leakey Foundation (to HMD and to BAP), the University of Southern California's URAP program (to BAP), the University of Southern California's Office of the Provost (to SMB), the Hill Foundation and the Baker Fund of the Department of Anthropology at the Pennsylvania Sate University (to HMD), the Research and Graduate Studies Office of the College of Liberal Arts at the Pennsylvania Sate University (to HMD), and the Pennsylvania Sate University Graduate School Alumni Association (to HMD).

Finally, HMD would specifically like to acknowledge Alan Walker for his assistance and guidance throughout the course of this study.

References

Anvari Z, Berillon G, Asgari Khaneghah A, Grimaud-Hervé D, Moulin V, Nicolas G. Kinematics and spatiotemporal parameters of infant-carrying in olive baboons. Am J Phys Anthropol. 2014; 155:392–404. [PubMed: 25059514]

Altmann, J. Baboon Mothers and Infants. Cambridge, MA: Harvard University Press; 2001.

Altmann J, Samuels A. Costs of maternal care, infant-carrying in baboons. Behav Ecol Sociobiol. 1992; 29:391–398.

Anvari Z, Berillon G, Asgari Khaneghah A, Grimaud-Hervé D, Moulin V, Nicolas G. Kinematics and spatiotemporal parameters of infant-carrying in olive baboons. Am J Phys Anthropol. 2014; 155:392–404. [PubMed: 25059514]

Bourne, GH. Collected anatomical and physiological data from the rhesus monkey. In: Bourne, GH., editor. The Rhesus Monkey, Volume 1, Anatomy and Physiology. New York: Academic Press; 1975. p. 1-63.

Boyer DM, Patel BA, Larson SG, Stern JT. Telemetered electromyography of peroneus longus in *Varecia variegata* and *Eulemur rubriventer*: implications for the functional significance of a large peroneal process. J Hum Evol. 2007; 53:119–134. [PubMed: 17349678]

Burr, DB., Organ, JM. Postcranial skeletal development and its evolutionary implications. In: Percival, CJ., Richtsmeier, JT., editors. Building Bones, Bone Formation and Development in Anthropology. Cambridge: Cambridge University Press; 2017. p. 148-174.

Brimacombe CS, Kuykendall KL, Nystrom P. Epiphyseal fusion in *Pan troglodytes* relative to dental age. Am J Phys Anthropol. 2015; 157:19–29. [PubMed: 25532866]

Byron C, Kunz H, Matuszek H, Lewis S, Van Valkinburgh D. Rudimentary pedal grasping in mice and implications for terminal branch arboreal quadrupedalism. J Morphol. 2011; 272:230–240. [PubMed: 21210492]

Byron CD, Herrel A, Pauwels E, Muynck AD, Patel BA. Mouse hallucal metatarsal cross-sectional geometry in a simulated fine branch niche. J Morphol. 2015; 276:759–765. [PubMed: 25758098]

Carlson KJ, Judex S. Increased non-linear locomotion alters diaphyseal bone shape. J Exp Biol. 2007; 210:3117–3125. [PubMed: 17704086]

Carlson KJ. Investigating the form-function interface in African apes: relationships between principal moments of area and positional behaviors in femoral and humeral diaphyses. Am J Phys Anthropol. 2005; 127:312–334. [PubMed: 15584067]

Cartmill, M. Pads and claws in arboreal locomotion. In: Jenkins, FA., Jr, editor. Primate Locomotion. New York: Academic Press; 1974. p. 45-83.

Cartmill, M. Climbing. In: Hidelbrand, M.Bramble, DM.Liem, KF., Wake, DB., editors. Functional Vertebrate Morphology. Cambridge, MA: Harvard University Press; 1985. p. 73-88.

Cheverud JM. Epiphyseal union and dental eruption in *Macaca mulatta*. Am J Phys Anthropol. 1981; 56:157–167. [PubMed: 7325218]

Congdon KA, Ravosa MJ. Get a grip, substrate orientation and digital grasping pressures in strepsirrhines. Folia Primatol. 2016; 87:224–243. [PubMed: 27794576]

Conroy GC, Rose MD. The evolution of the primate foot from the earliest primates to the Miocene hominoids. Foot Ankle. 1983; 3:342–364. [PubMed: 6409714]

Dean MC, Wood BA. Developing pongid dentition and its use for aging individual crania in comparative cross-sectional growth studies. Folia Primatol. 1981; 36:111–127. [PubMed: 7338332]

Demes B, Larson SG, Stern JT, Jungers WL, Biknevicius AR, Schmitt D. The kinetics of primate quadrupedalism, " hindlimb drive" reconsidered. J Hum Evol. 1994; 26:353–374.

Doran DM. The ontogeny of chimpanzee and pygmy chimpanzee locomotor behavior - a case-study of paedomorphism and its behavioral correlates. J Hum Evol. 1992; 23:139–157.

Doran DM. Ontogeny of locomotion in mountain gorillas and chimpanzees. J Hum Evol. 1997; 32:323–344. [PubMed: 9085185]

Doube M, Kłosowski MM, Arganda-Carreras I, et al. BoneJ: free and extensible bone image analysis in ImageJ. Bone. 2010; 47:1076–1079. [PubMed: 20817052]

Dowdeswell MR, Jashashvili T, Patel BA, et al. Adaptation to bipedal gait and fifth metatarsal structural properties *Australopithecus*, *Paranthropus*, and *Homo*. C R Palevol. (in press).

Dunbar, DC. Physical anthropology at the Caribbean Primate Research Center: past, present and future. In: Wang, Q., editor. Bone, Genetics, and Behavior of Rhesus Macaques. New York: Springer; 2012. p. 1-35.

Dunsworth, HM. *Proconsul heseloni* feet from Rusinga Island, Kenya. Pennsylvania State University; 2006. Ph D Dissertation

Fragaszy DM, Adams-Curtis LE, Baer JF, Carlson-Lammers R. Forelimb dimensions and goniometry of the wrist and fingers in tufted capuchin monkeys (*Cebus apella*): developmental and comparative aspects. Am J Primatol. 1989; 17:133–146.

Gebo D. The nature of the primate grasping foot. Am J Phys Anthropol. 1985; 67:269–277.

Goodenberger KE, Boyer DM, Orr CM, Jacobs RL, Femiani JC, Patel BA. Functional morphology of the hallucal metatarsal with implications for inferring grasping ability in extinct primates. Am J Phys Anthropol. 2015; 156:327–348. [PubMed: 25378276]

Grand TI. Body weight: its relation to tissue composition, segment distribution, and motor function. II. Development of *Macaca mulatta*. Am J Phys Anthropol. 1977; 47:241–248. [PubMed: 410306]

Griffin NL, Richmond BG. Cross-sectional geometry of the human forefoot. Bone. 2005; 37:253–260. [PubMed: 15963776]

Higurashi Y, Hirasaki E, Kumakura H. Palmar and plantar pressure while walking on a horizontal ladder and single pole in *Macaca fuscata*. Int J Primatol. 2010; 31:181–190.

Hirasaki E, Higurashi Y, Kumakura H. Brief communication: dynamic plantar pressure distribution during locomotion in Japanese macaques (*Macaca fuscata*). Am J Phys Anthropol. 2010; 142:149–156. [PubMed: 20027608]

Jashashvili T, Dowdeswell MR, Lebrun R, Carlson KJ. Cortical structure of hallucal metatarsals and locomotor adaptations in hominoids. PLoS ONE. 2015; 10(1):e0117905. [PubMed: 25635768]

Jepsen KJ, Hu B, Tommasini SM, et al. Phenotypic integration of skeletal traits during growth buffers genetic variants affecting the slenderness of femora in inbred mouse strains. Mamm Genome. 2009; 20:21–33. [PubMed: 19082857]

Jungers WL, Fleagle JG. Postnatal growth allometry of the extremities in *Cebus albifrons* and *Cebus apella*: a longitudinal and comparative study. Am J Phys Anthropol. 1980; 53:471–478. [PubMed: 7468784]

Kenney, EB. Development and eruption of teeth in Rhesus. In: Bourne, GH., editor. The Rhesus Monkey, Volume 1, Anatomy and Physiology. New York: Academic Press; 1975. p. 145-167.

Kingston AK, Boyer DM, Patel BA, Larson SG, Stern JT. Hallucal grasping in N*ycticebus coucang*: further implications for the functional significance of a large peroneal process. J Hum Evol. 2010; 58:33–42. [PubMed: 19800655]

Lieberman DE, Polk JD, Demes B. Predicting long bone loading from cross-sectional geometry. Am J Phys Anthropol. 2004; 123:156–171. [PubMed: 14730649]

Marchi D. The cross-sectional geometry of the hand and foot bones of the hominoidea and its relationship to locomotor behavior. J Hum Evol. 2005; 49:743–761. [PubMed: 16219337]

Marchi D. Articular to diaphyseal proportions of human and great ape metatarsals. Am J Phys Anthropol. 2010; 143:198–207. [PubMed: 20853475]

Nakamichi M, Yamada K. Distribution of dorsal carriage among simians. Primates. 2009; 50:153–168. [PubMed: 19274474]

O'Neill MC, Ruff CB. Estimating human long bone cross-sectional geometric properties, a comparison of noninvasive methods. J Hum Evol. 2004; 47:221–235. [PubMed: 15454334]

Organ JM. Structure and function of platyrrhine caudal vertebrae. Anat Rec. 2010; 293:730–745.

Patel BA, Larson SG, Stern JT. Electromyography of crural and pedal muscles in tufted capuchin monkeys (*Sapajus apella*): implications for hallucal grasping behavior and first metatarsal morphology in euprimates. Am J Phys Anthropol. 2015a; 156:553–564. [PubMed: 25693754]

Patel BA, Wallace IJ, Boyer DM, Granatosky MC, Larson SG, Stern JT. Distinct functional roles of primate grasping hands and feet during arboreal quadrupedal locomotion. J Hum Evol. 2015b; 88:79–84. [PubMed: 26553820]

Patel BA, Ruff CB, Simons ELR, Organ JM. Humeral cross-sectional shape in suspensory primates and sloths. Anat Rec. 2013; 296:545–556.

Patel BA, Yapuncich GS, Tran C, Nengo IO. Catarrhine hallucal metatarsals from the early Miocene site of Songhor, Kenya. J Hum Evol. 2017; 108:176–198. [PubMed: 28622929]

Polk J, Demes B, Jungers W, Biknevicius A, Heinrich R, Runestad J. A comparison of primate, carnivoran and rodent limb bone cross-sectional properties: are primates really unique? J Hum Evol. 2000; 39:297–325. [PubMed: 10964531]

Preuschoft, H. The functional anatomy of the lower extremity. In: Bourne, GH., editor. The Chimpanzee. Vol. 3. Basel: Karger; 1970. p. 221-294.Immunology, Infections, Hormones, Anatomy and behavior

Raichlen DA. Effects of limb mass distribution on the ontogeny of quadrupedalism in infant baboons (*Papio cynocephalus*) and implications for the evolution of primate quadrupedalism. J Hum Evol. 2005; 49:415–431. [PubMed: 15998533]

Rasband, WS. ImageJ. U. S. National Institutes of Health; Bethesda, Maryland, USA: 1997–2016. http//imagej.nih.gov/ij/

Rawlins, RG. Locomotor ontogeny of the Cayo Santiago macaques: a behavioral and morphological analysis. Google Books/Google Play; 1982. self-published

Rawlins, RG., Kessler, MJ. Demography of the free-ranging Cayo Santiago macaques 1976–1983. In: Rawlins, RG., Kessler, MJ., editors. The Cayo Santiago Macaques. Albany, NY: State University of New York Press; 1986. p. 47-72.

Roberts TJ, Gabaldón AM. Interpreting muscle function from EMG, lessons learned from direct measurements of muscle force. Int Comp Bio. 2008; 48:312–320.

Ross C. Park or ride? Evolution of infant carrying in primates. Int J Primatol. 2001; 22:749–771.

Ruff CB. Body size, body shape, and long bone strength in modern humans. J Hum Evol. 2000; 38:269–290. [PubMed: 10656779]

Ruff CB. Long bone articular and diaphyseal structure in Old World monkeys and apes. II: estimation of body mass. Am J Phys Anthropol. 2003a; 120:16–37. [PubMed: 12489135]

Ruff C. Ontogenetic adaptation to bipedalism, age changes in femoral to humeral length and strength proportions in humans, with a comparison to baboons. J Hum Evol. 2003b; 45:317–349. [PubMed: 14585245]

Ruff CB, Hayes WC. Cross-sectional geometry of Pecos Pueblo femora and tibiae - a biomechanical investigation: I. method and general patterns of variation. Am J Phys Anthropol. 1983; 60:359–381. [PubMed: 6846510]

Russo GA, Young JW. Tail growth tracks the ontogeny of prehensile tail use in capuchin monkeys (*Cebus albifrons* and *C. apella*). Am J Phys Anthropol. 2011; 146:465–473. [PubMed: 21953012]

Sarringhaus LA, MacLatchy LM, Mitani JC. Locomotor and postural development of wild chimpanzees. J Hum Evol. 2014; 66:29–38. [PubMed: 24238359]

Sarringhaus LA, MacLatchy LM, Mitani JC. Long bone cross-sectional properties reflect changes in locomotor behavior in developing chimpanzees. Am J Phys Anthropol. 2016; 160:16–29. [PubMed: 26780478]

Smith BH, Crummett TL, Brandt KL. Ages of eruption on primate teeth: a compendium for aging individuals and comparing life histories. Yearb Phys Anthropol. 1994; 37:177–231.

Smith BH, Boesch C. Mortality and the magnitude of the “wild effect” in chimpanzee tooth emergence. J Hum Evol. 2011; 60:34–46. [PubMed: 21071064]

Smith RJ, Jungers WL. Body mass in comparative primatology. J Hum Evol. 1997; 32:523–559. [PubMed: 9210017]

Smith TM, Machanda Z, Bernard AB, et al. First molar eruption, weaning, and life history in living wild chimpanzees. PNAS. 2013; 110:2787–2791. [PubMed: 23359695]

Stock JT. A test of two methods of radiographically deriving long bone cross-sectional properties compared to direct sectioning of the diaphysis. Int J Osteoarchaeol. 2002; 12:335–342.

Strasser E. Relative development of the hallux and pedal digit formulae in Cercopithecidae. J Hum Evol. 1994; 26:413–440.

Szalay F, Dagosto M. Evolution of hallucial grasping in the primates. J Hum Evol. 1988; 17:1–33.

Vereecke E, D’Août K, De Clercq D, Van Elsacker L, Aerts P. Dynamic plantar pressure distribution during terrestrial locomotion of bonobos (*Pan paniscus*). Am J Phys Anthropol. 2003; 120:373–383. [PubMed: 12627532]

Wallace IJ, Tommasini SM, Judex S, Garland T, Demes B. Genetic variations and physical activity as determinants of limb bone morphology, an experimental approach using a mouse model. Am J Phys Anthropol. 2012; 148:24–35. [PubMed: 22331623]

Wells JP, Turnquist JE. Ontogeny of locomotion in rhesus macaques (*Macaca mulatta*): II. postural and locomotor behavior and habitat use in a free-ranging colony. Am J Phys Anthropol. 2001; 115:80–94. [PubMed: 11309753]

Wunderlich, RE. Ph.D. Dissertation. SUNY Stony Brook; 1999. Pedal form and plantar pressure distribution in anthropoid primates.

Wunderlich RE, Ischinger SB. Foot use during vertical climbing in chimpanzees (*Pan troglodytes*). J Hum Evol. 2017; 109:1–10. [PubMed: 28688455]

Young JW, Fernández D, Fleagle JG. Ontogeny of long bone geometry in capuchin monkeys (*Cebus albifrons* and *Cebus apella*): implications for locomotor development and life history. Biol Lett. 2010; 6:197–200. [PubMed: 19864273]

Young JW, Heard-Booth AN. Grasping primate development: ontogeny of intrinsic hand and foot proportions in capuchin monkeys (*Cebus albifrons* and *Sapajus apella*). Am J Phys Anthropol. 2016; 161:104–115. [PubMed: 27324663]

Zihlman AL, Bolter DR, Boesch C. Skeletal and dental growth and development in chimpanzees of the Taï National Park, Côte D'Ivoire. J Zool. 2007; 273:63–73.

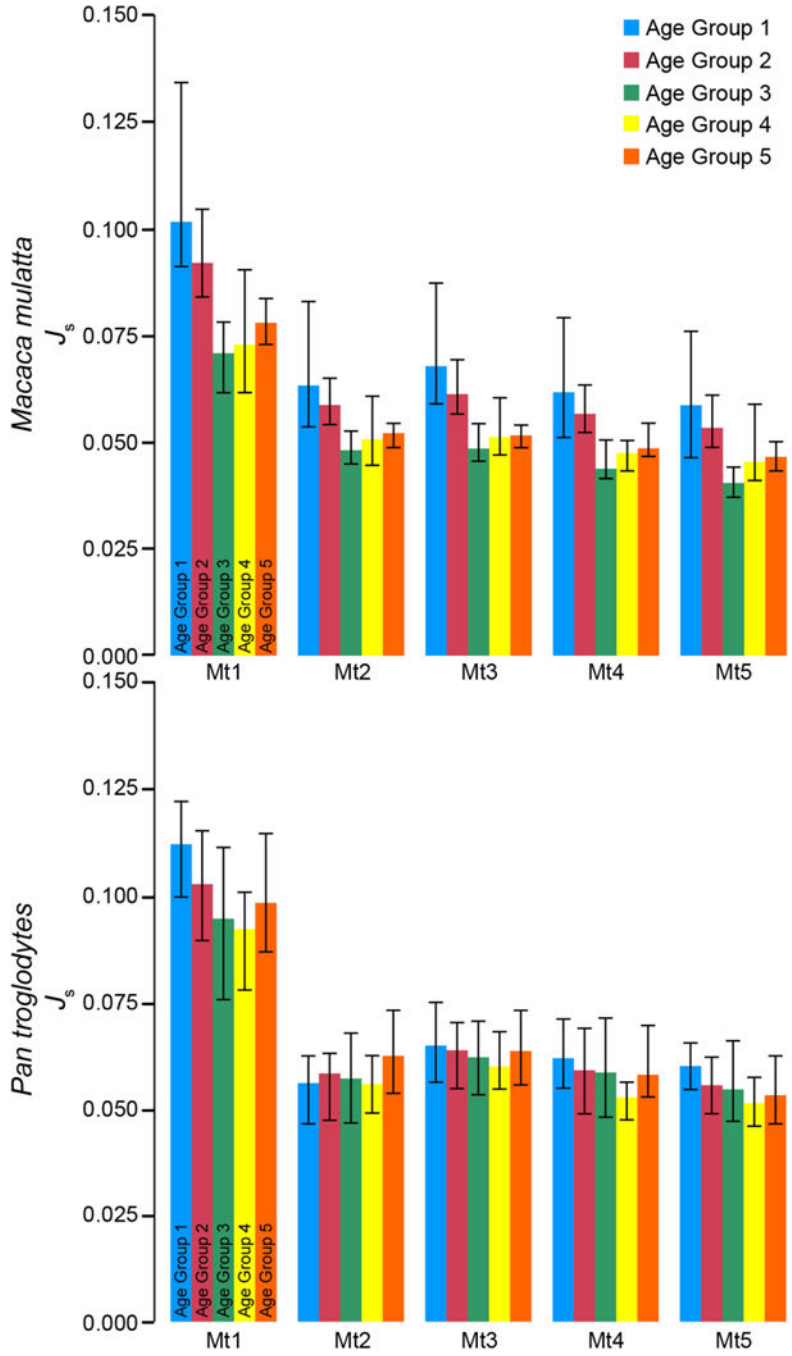

Fig. 1.

Bar plots of relative rigidity, J_s (= $J^{0.25}/L$), within metatarsals (Mt) and across age groups in rhesus macaque (*Macaca mulatta*; top) and chimpanzees (*Pan troglodytes*; bottom). Bars represent mean values and whiskers show the total range. Age groups defined in Table 1.

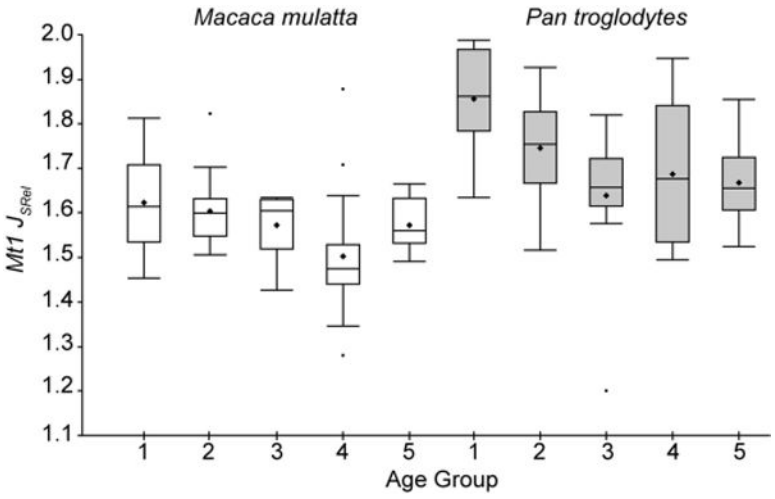

Fig 2.

Box-and-whiskers plots of Mt1 J_{SRel} (= Mt1 J_s/[Mt2–5 J_s]$^{0.25}$) across age groups in rhesus macaques (*Macaca mulatta*; white boxes) and chimpanzees (*Pan troglodytes*; grey boxes. Filled diamonds within each box indicate mean values. Horizontal lines within each box illustrate the median of the distribution. Boxes envelop the inter quartile range (50% of values) of the sample distribution, and whiskers encompass the range excluding outliers. Filled circles beyond whiskers indicate outliers. Age groups defined in Table 1.

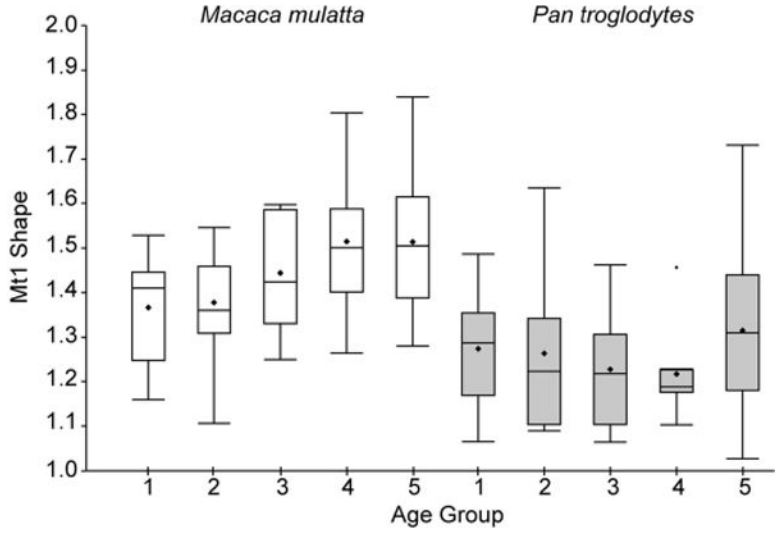

Fig 3.

Box-and-whiskers plots of Mt1 shape (= *Imax/Imin* ratio) across age groups in rhesus macaques (*Macaca mulatta*; white boxes) and chimpanzees (*Pan troglodytes*; grey boxes). Filled diamonds within each box indicate mean values. Horizontal lines within each box illustrate the median of the distribution. Boxes envelop the inter quartile range (50% of values) of the sample distribution, and whiskers encompass the range excluding outliers. Filled circles beyond whiskers indicate outliers. Age groups defined in Table 1.

Table 1

Ontogenetic age groups definitions in rhesus macaques (*Macaca*) and chimpanzees (*Pan*).

Ontogenetic age group	Tooth eruption stage	*Macaca* age ranges (years)[#]	*Pan* age ranges (years)[†]	Locomotor stage[‡]
1	Only deciduous teeth visible	<1	<3	Not independent
2	M1 erupting	1–2.5	3–5	Transitional
3	M1 fully erupted and M2 erupting	2.5–4.5	5–10	Independent
4	M2 fully erupted and M3 erupting	4.5–7	10–15	Independent
5	All teeth in occlusion	>7	>15	Independent

[#]Following Kenny (1975).

[†]Following Sarringhaus et al. (2016) with data from Smith et al. (1994), Smith and Boesch (2011), and Smith et al. (2013).

[‡]Based on data from Doran (1997), Wells and Turnquist (2001), and Sarringhaus et al. (2016).

Table 2

Descriptive statistics for metatarsal variables in rhesus macaques (*Macaca*) and chimpanzees (*Pan*) across five age groups.[#]

Variable	Taxon	Age Group	n	Mt1		Mt2		Mt3		Mt4		Mt5	
				Mean	1 SD	Mean	1 SD	Mean	1 SD	Mean	1 SD	Mean	1 SD
L (mm)	*Macaca*	1	11	17.23	2.57	23.89	4.54	25.12	4.51	24.84	4.54	22.80	4.36
		2	16	22.24	2.43	32.19	3.92	33.71	4.20	33.79	4.19	31.93	4.53
		3	7	34.21	3.43	49.67	4.72	52.01	4.91	52.39	4.73	49.83	4.50
		4	23	34.75	2.46	50.17	3.34	52.98	3.85	53.16	3.76	50.94	3.79
		5	16	31.31	2.65	47.57	3.97	50.62	4.15	50.97	3.89	48.17	4.52
	Pan	1	13	27.81	2.96	37.82	4.89	35.22	3.94	33.77	3.50	31.71	3.73
		2	15	38.47	4.73	51.01	4.87	47.81	5.34	46.48	5.48	45.58	5.64
		3	12	48.77	8.77	63.24	7.43	58.52	8.03	55.76	8.17	55.61	8.92
		4	8	54.12	3.88	73.02	5.78	67.20	5.83	66.28	4.87	65.14	5.06
		5	32	54.85	3.28	72.97	4.49	68.77	4.33	66.67	4.12	66.84	4.18
J (mm^4)	*Macaca*	1	11	9.18	3.09	5.12	2.27	8.13	2.87	5.32	1.98	3.09	1.36
		2	16	17.90	6.03	13.58	6.43	18.51	6.40	13.96	5.59	8.86	4.47
		3	7	35.65	15.77	34.25	17.35	41.91	18.70	28.19	10.18	18.03	11.08
		4	23	42.36	14.20	43.82	17.15	54.94	16.15	41.79	13.69	30.08	11.90
		5	16	36.97	13.05	39.35	14.27	48.12	16.97	38.91	13.69	26.88	11.50
	Pan	1	13	96.20	34.10	20.52	8.94	27.92	11.36	20.76	12.60	13.17	4.09
		2	15	252.62	115.27	84.85	47.00	91.24	49.11	59.20	29.46	44.40	25.90
		3	12	433.29	131.15	176.51	71.78	175.08	68.38	123.51	83.26	89.72	47.82
		4	8	629.60	209.40	278.30	95.36	269.55	107.08	151.39	54.26	131.52	68.15
		5	32	866.66	272.74	440.84	159.88	368.99	107.14	226.39	69.36	162.81	50.10
J_s	*Macaca*	1	11	0.101	0.013	0.063	0.009	0.068	0.009	0.062	0.008	0.059	0.008
		2	16	0.092	0.007	0.059	0.003	0.061	0.004	0.057	0.003	0.053	0.004
		3	7	0.071	0.005	0.048	0.003	0.048	0.003	0.044	0.003	0.040	0.002
		4	23	0.073	0.005	0.051	0.004	0.051	0.003	0.047	0.002	0.045	0.004
		5	16	0.068	0.002	0.048	0.001	0.048	0.001	0.046	0.002	0.043	0.002
	Pan	1	13	0.112	0.007	0.056	0.004	0.065	0.005	0.062	0.005	0.060	0.004

Variable	Taxon	Age Group	n	Mt1		Mt2		Mt3		Mt4		Mt5	
				Mean	1 SD	Mean	1 SD	Mean	1 SD	Mean	1 SD	Mean	1 SD
		2	15	0.103	0.007	0.058	0.005	0.064	0.004	0.059	0.005	0.055	0.004
		3	12	0.094	0.011	0.057	0.006	0.062	0.006	0.058	0.007	0.054	0.005
		4	8	0.092	0.009	0.056	0.004	0.060	0.005	0.052	0.003	0.051	0.003
		5	32	0.098	0.007	0.062	0.005	0.063	0.004	0.058	0.004	0.053	0.003

[#] L, length; J, polar moment of area; $J_S = J^{0.25}/L$; Mt, metatarsal; n, sample size; SD, standard deviation.

Table 3

Results of ANOVAs and post-hoc tests comparing J_s across five age groups for each metatarsal in rhesus macaques (*Macaca*) and chimpanzees (*Pan*).[#]

Taxon	Bone	ANOVA results		Tukey's HSD *p* value			
Macaca	**M1**	***p*<0.0001***	**Age Group**	**2**	**3**	**4**	**5**
		F=44.56	1	**0.0078***	**<0.0001***	**<0.0001***	**<0.0001***
			2		**<0.0001***	**<0.0001***	**<0.0001***
			3			0.9652	0.1826
			4				0.1809
Pan	Mt1	***p*<0.0001***	Age Group	2	3	4	5
		F=12.15	1	**0.0175***	**<0.0001***	**<0.0001***	**<0.0001***
			2		0.0649	**0.0224***	0.3772
			3			0.9586	0.6246
			4				0.2763
Macaca	Mt2	***p*<0.0001***	Age Group	2	3	4	5
		F=23.89	1	0.0669	**<0.0001***	**<0.0001***	**<0.0001***
			2		**<0.0001***	**<0.0001***	**0.0007***
			3			0.6560	0.2728
			4				0.8565
Pan	Mt2	***p*<0.0001***	Age Group	2	3	4	5
		F=6.32	1	0.7528	0.9983	0.9999	**0.0021***
			2		0.9181	0.7953	0.0769
			3			0.9971	**0.0127***
			4				**.01200***
Macaca	Mt3	***p*<0.0001***	Age Group	2	3	4	5
		F=42.45	1	**0.0025***	**<0.0001***	**<0.0001***	**<0.0001***
			2		**<0.0001***	**<0.0001***	**<0.0001***
			3			0.6084	0.5240
			4				0.9986

Taxon	Bone	ANOVA results	Tukey's HSD *p* value				
Macaca	**M1**	***p*<0.0001***	**Age Group**	**2**	**3**	**4**	**5**
Pan	Mt3	***p*=0.0003***	Age Group	2	3	4	5
		F=1.81	1	0.7536	0.983	0.9999	**0.0021***
			2		0.9726	0.796	0.0774
			3			0.9812	**0.0209***
			4				**0.0121***
Macaca	Mt4	***p*<0.0001***	Age Group	2	3	4	5
		F=43.75	1	**0.0085***	**<0.0001***	**<0.0001***	**<0.0001***
			2		**<0.0001***	**<0.0001***	**<0.0001***
			3			0.1749	0.0521
			4				0.8970
Pan	Mt4	***p*=0.0013***	Age Group	2	3	4	5
		F=4.97	1	0.5007	0.3837	**0.0003***	0.0917
			2		0.9985	**0.0208***	0.9478
			3			0.0559	0.9968
			4				**0.0405***
Macaca	Mt5	***p*<0.0001***	Age Group	2	3	4	5
		F=34.11	1	**0.0241***	**<0.0001***	**<0.0001***	**<0.0001***
			2		**<0.0001***	**<0.0001***	**0.0004***
			3			0.0871	**0.0280***
			4				0.9298
Pan	Mt5	***p*<0.0001***	Age Group	2	3	4	5
		F=9.35	1	**0.0217***	**0.0052***	**<0.0001***	**<0.0001***
			2		0.0963	0.0987	0.2892
			3			0.3567	0.8260
			4				0.7393

#$J_S = J^{0.25}/L$, where L is length (mm) and J is polar moment of area (mm^4); Mt, metatarsal.

Author Manuscript

Author Manuscript

Author Manuscript

* **Bold** values significant at the $p<0.05$.

Table 4

Results of ANOVAs comparing J_S between rhesus macaques and chimpanzees in five age groups and five metatarsals.[#†]

Bone	Age Group 1	Age Group 2	Age Group 3	Age Group 4	Age Group 5
Mt1	**0.0235**[*]	**0.0002**[*]	**<0.0001**[*]	**<0.0001**[*]	**<0.0001**[*]
	P>M	P>M	P>M	P>M	P>M
Mt2	**0.0138**[*]	0.7457	**0.0010**[*]	**0.0042**[*]	**<0.0001**[*]
	M>P	M>P	P>M	P>M	P>M
Mt3	0.2732	0.12	**<0.0001**[*]	**<0.0001**[*]	**<0.0001**[*]
	M>P	P>M	P>M	P>M	P>M
Mt4	0.9851	0.1435	**<0.0001**[*]	**<0.0001**[*]	**<0.0001**[*]
	P>M	P>M	P>M	P>M	P>M
Mt5	0.6124	0.1619	**<0.0001**[*]	**0.0005**[*]	**<0.0001**[*]
	P>M	P>M	P>M	P>M	P>M

[#] $J_S = J^{0.25}/L$, where J is polar moment of area (mm^4) and L is length (mm); Mt, metatarsal; M, rhesus macaque; P, chimpanzee.

[†] p value above; size difference below (e.g., P>M = chimpanzee values greater than macaque values).

[*] **Bold** values significant at the $p<0.05$.

Table 5

Results of RMA regression analyses between metatarsal *L* and *J* in rhesus macaques (*Macaca*) and chimpanzees (*Pan*).[#]

Taxon	Bone	Slope	95% CI[†]	Intercept	r^2	*p*	Allometry[‡]
Macaca	Mt1	2.3073	2.0742–2.5385	−4.4274	0.8385	**<0.001**[*]	negative
	Mt2	2.9159	2.6541–3.1708	−7.6812	0.9112	**<0.001**[*]	negative
	Mt3	2.5298	2.3226–2.7185	−6.0924	0.9213	**<0.001**[*]	negative
	Mt4	2.6736	2.4491–2.8579	−6.9406	0.9189	**<0.001**[*]	negative
	Mt5	2.8319	2.5631–3.0680	−7.1800	0.8853	**<0.001**[*]	negative
Pan	Mt1	3.1863	2.9620–3.3989	−6.1336	0.8927	**<0.001**[*]	negative
	Mt2	4.5089	4.1745–4.8052	−13.4240	0.8979	**<0.001**[*]	positive
	Mt3	3.8068	3.5854–4.0044	−10.2920	0.9219	**<0.001**[*]	isometry
	Mt4	3.6489	3.4459–3.8590	−9.9923	0.8981	**<0.001**[*]	negative
	Mt5	3.4175	3.2215–3.5831	−9.3321	0.9335	**<0.001**[*]	negative

[#]RMA, reduced major axis; Mt, metatarsal; *L*, length (mm); *J*, polar moment of area (mm^4).

[†]CI: confidence interval of slope.

[‡]Slope of 4.0 expected for isometry.

[*]**Bold** values significant at the $p<0.05$.

Table 6

Descriptive statistics for Mt1 J_{SRel} in rhesus macaques (*Macaca*) and chimpanzees (*Pan*) across five age groups.[#]

Taxon	Age Group	n	Mean	1 SD
Macaca	1	11	1.623	0.111
	2	16	1.604	0.078
	3	7	1.573	0.076
	4	23	1.503	0.122
	5	16	1.573	0.056
Pan	1	13	1.856	0.110
	2	15	1.745	0.108
	3	12	1.639	0.154
	4	8	1.687	0.162
	5	32	1.667	0.083

[#] J_{SRel} = Mt1 J_S/[Mt2–5 J_S]$^{0.25}$, where $J_S = J^{0.25}/L$ and where J is polar moment of area (mm^4) and L is length (mm); Mt, metatarsal; n, sample size; SD, standard deviation.

Table 7

Results of ANOVAs and post-hoc tests comparing Mt1 J_{SRel} across five age groups in rhesus macaques (*Macaca*) and chimpanzees (*Pan*).[#]

Taxon	ANOVA results	Tukey's HSD *p* value				
Macaca	***p*=0.0047**[*]	**Age Group**	**2**	**3**	**4**	**5**
	F=4.135	1	0.9867	0.8109	**0.0090**[*]	0.6652
		2		0.9494	**0.0151**[*]	0.8844
		3			0.4493	0.9999
		4				0.1783
Pan	*p*<**0.0001**[*]	Age Group	2	3	4	5
	F=8.120	1	0.0847	<**0.0001**[*]	**0.0120**[*]	<**0.0001**[*]
		2		0.1234	0.7683	0.1947
		3			0.8866	0.9477
		4				0.9922

[#] J_{SRel} = Mt1 J_S/[Mt2–5 J_S]$^{0.25}$, where $J_S = J^{0.25}/L$ and where J is polar moment of area (mm^4) and L is length (mm); Mt, metatarsal.

[*] **Bold** values significant at the $p<0.05$.

Table 8

Results of ANOVAs comparing Mt1 J_{SRel} between rhesus macaques and chimpanzees in five age groups.[#]

Age Group	F	*p*	Directional difference[†]
1	26.592	**<0.0001**[*]	P>M
2	17.398	**0.0003**[*]	P>M
3	1.247	0.3037	P>M
4	11.414	**0.0021**[*]	P>M
5	16.861	**0.0002**[*]	P>M

[#] J_{SRel} = Mt1 J_S/[Mt2–5 J_S]$^{0.25}$, where $J_S = J^{0.25}/L$ and where J is polar moment of area (mm^4) and L is length (mm); Mt, metatarsal; M, rhesus macaque; P, chimpanzee.

[†] P>M = chimpanzee values greater than macaque values.

[*] **Bold** values significant at the $p<0.05$.

Table 9

Descriptive statistics for Mt1 Shape (=*Imax*/I*min*) in rhesus macaques (*Macaca*) and chimpanzees (*Pan*) across five age groups.[#]

Taxon	Age Group	n	Mean	1 SD
Macaca	1	11	1.367	1.220
	2	16	1.378	1.109
	3	7	1.444	1.281
	4	23	1.515	1.523
	5	16	1.514	1.651
Pan	1	13	1.274	1.219
	2	15	1.264	1.831
	3	12	1.228	1.238
	4	8	1.218	1.038
	5	32	1.315	1.692

[#]Mt, metatarsal; n, sample size; SD, standard deviation.

Table 10

Results of ANOVAs and post-hoc tests7 comparing Mt1 Shape (=*Imax*/*Imin*) across five age groups in rhesus macaques (*Macaca*) and chimpanzees (*Pan*).[#]

Taxon	ANOVA results	Tukey's HSD *p* value				
Macaca	***p*=0.0054***	**Age Group**	**2**	**3**	**4**	**5**
	F=4.040	1	0.9996	0.7850	**0.0417***	0.0688
		2		0.8361	**0.0307***	0.0592
		3			0.7715	0.8091
		4				0.9999
Pan	*p*=0.3485	Age Group	2	3	4	5
	F=1.130	1	0.9998	0.9425	0.9244	0.9258
		2		0.9740	0.9595	0.8199
		3			0.9999	0.4506
		4				0.4982

[#]Mt, metatarsal.

*__Bold__ values significant at the $p<0.05$